Enhanced LIGO HAM ISI Prototype
Preliminary Performance Review
T-080251-01

Jeff Kissel, Brian Lantz

October 7, 2008

Abstract

As of May 2008, both L1 and H1 interferometers have had an active seismic isolation system installed in their respective sixth HAM chamber. During the month of June, other members of the SEI team and I performed the bulk of the commissioning effort on the active seismic isolation system, or HAM ISI. This document reviews the results from those commissioning efforts.

1 Introduction

The Horizontal Access Module In-vacuum Seismic Isolation system (HAM ISI) is a single stage active isolation and alignment platform to be used in the Advanced LIGO. Two prototypes of these platforms, one for each 4 km interferometer, have been constructed and installed as of May 2008 for the precursory Enhanced LIGO upgrade. In this document we will describe the active portion of the table, and detailing the initial performance with respect to Advanced LIGO requirements.

1.1 The Isolation Loop

Figure 1 shows a schematic of the overall loop structure. There are two loops in the control design, damping loops and isolation loops. The damping loops are six single-input, single output (SISO) loops from the individual inertial sensors to their colocated actuators (the green path in Figure 1). The purpose of these loops is to reduce the Q of 0.8 to 1.8 Hz translational resonant modes in the blade spring flexure suspension system. These loops provide a simple, stable plant for the isolation loops that is robust against perturbations, unconditionally stable, but with gain only around the resonant modes of the suspended stage.

The isolation path uses both displacement and inertial sensor information to isolate the platform from ground motion with an upper unity gain frequency of over 25 Hz. This path (following green and blue paths in Figure 1) is where measurable performance occurs. The software implemented for isolation loops is as follows (moving counter-clockwise from the HAM ISI plant).

Basis Conversion Matrices The sensor array measures the table in the colocated basis. However, since the isolation filters are designed to control the coordinate basis degrees of freedom, a basis transformation must be performed. This block, which is simply a gain matrix, performs the necessary transformation.

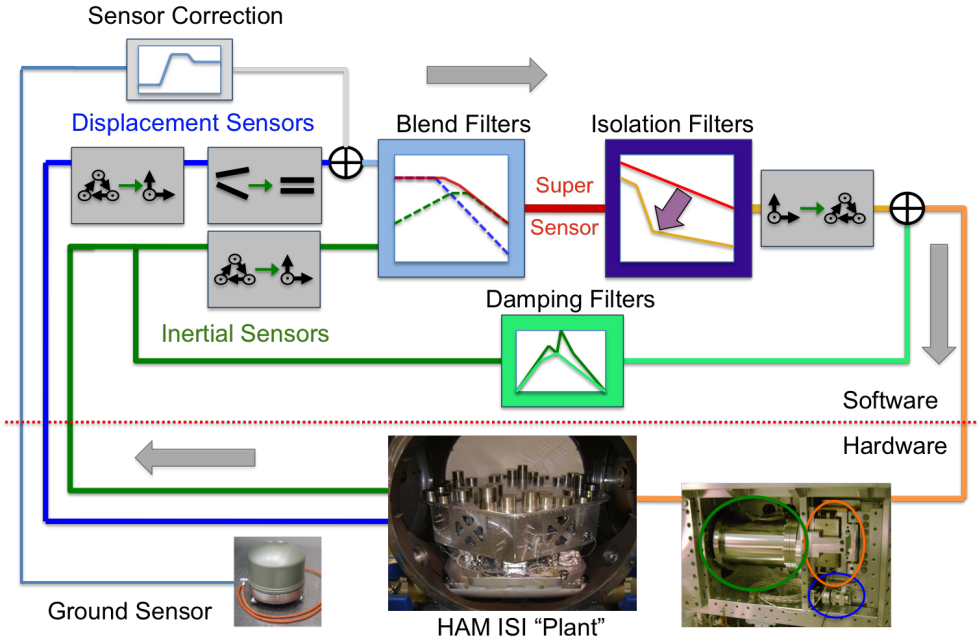

Figure 1: Control loop structure for the HAM ISI active isolation.

Displacement Sensor Alignment Though very little tolerance was allowed for the plates in the displacement sensors, there is no guarantee they are exactly parallel in the construction of the platform. Any misalignment may send false tilt information to the control loops, which in turn increases the frequency at which the GEOs can no longer distinguish between tilt and velocity. In the ideal case, this DISP sensor gain matrix would be a six-dimensional identity matrix, i.e. the X displacement sensor shows only X motion. In practice the translational degrees of freedom produce rotational signal in misaligned DISPs at the tenth of a percent level, hence off diagonal gains must be put in place.

Blend Filters To be isolated from ground, the platform should not move in inertial space. However, the payload of the platform is part of an interferometer, which must be aligned at some DC level. At and near DC, inertial sensors are dominated by tilt noise and readout electronic noise. Hence the inertial sensor signals are blended with displacement sensors where which are unaffected by tilt, and designed to measure platform motion at such low frequencies. The crossover frequency where these signals are mixed depends on the tilt-horizontal coupling frequency, and the noise performance of each sensor. The resulting signal from the blended sensors, or "supersensor" is used as the plant measurement for the isolation filters.

Isolation Filters These filters control platform motion over a large range of frequencies ($\sim$ 25 Hz down to DC). They drive the suspended stage, holding it in inertial space in the coordinate degrees of freedom, remove higher frequency bending resonances, and have high gain at low frequencies. These aggressive filters are designed only as conditionally stable. Further guidelines for the design of these filters are detailed below.

Sensor Correction The displacement sensors measure relative motion between the support stage and the suspended stage. Since the support stage is attached to the ground, this means that they are sensitive to motion of the suspended stage *and ground motion*. Once the high gain isolation loops are in place, this noise dominates at low frequency because of the shape of the displacement sensor blend filter. If a sensitive inertial sensor is set up on the ground independently measuring ground motion, its signal can be fed forward to correct for ground motion in the displacement sensor.

1.2 Requirements

The displacement requirements for the HAM ISI are detailed in T060075-00-D, but can be summarized as 2e-11 m/rtHz at 10Hz; increasing as $1/f$ below 10 Hz until about 0.6 Hz; increase as f^{-4} below 0.6 Hz until 0.2 Hz where it must return back to $1/f$. These requirements are plotted in Figure 2.

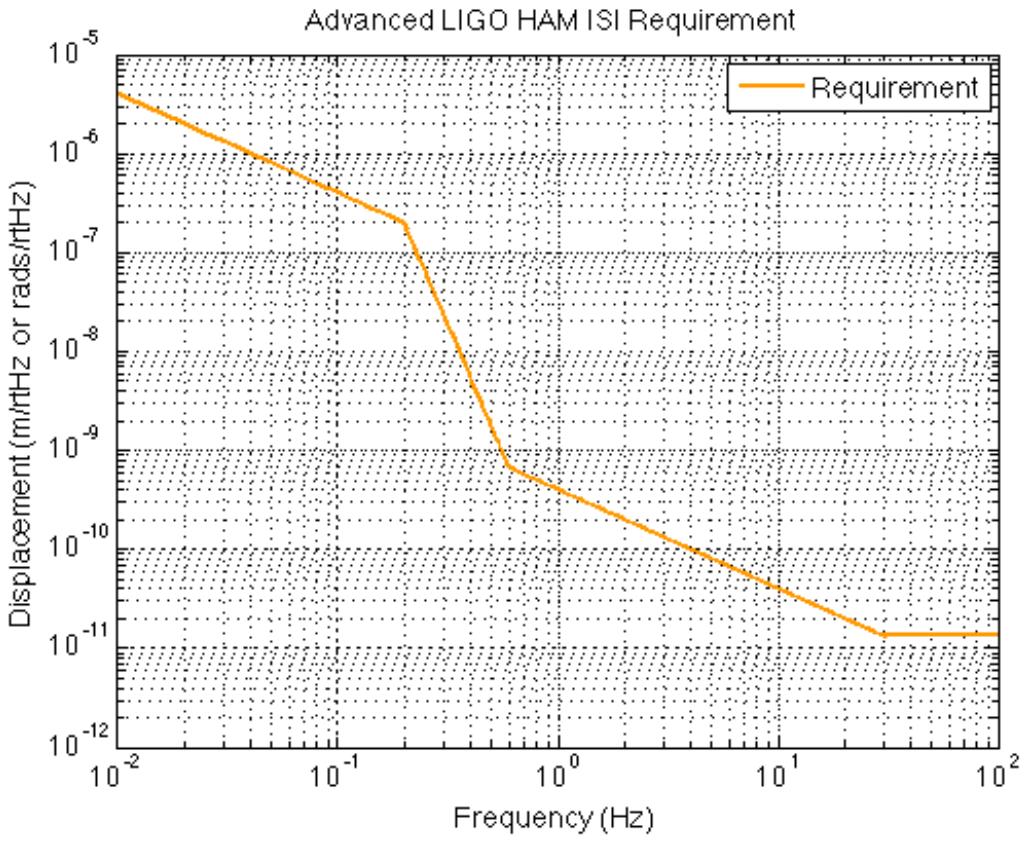

Figure 2: Advanced LIGO motion requirements for the HAM ISI.

1.3 Goals

These requirements described in Section 1.2 are estimates. A detailed requirement of suspensions and optic performance might might need to focus on a particular area of isolation. After we get a better idea of what each chamber/optic needs, it will be possible (and in fact recommended) to tweak the performance here and there; trade isolation in some areas for that in others. In the absence of such goals, we're currently designing loops that do a "good" job in all areas. The guidelines for our design (in no particular order of importance) are:

- Design the RX and RY isolation loops first, such that one takes as much tilt out of the plant as possible before designing the X, Y, Z, and RZ isolation loops.
- Shoot for a unity gain frequency (UGF) of 25 Hz. From my experience with H1's HAM6 ISI, this guideline is always met and often pushed higher. The highest we've been able to go is 30 Hz (L1's HAM ISI, in RX; entry to follow)
- With no low-frequency boost, we prefer no DC poles (integraters) in the isolation loops. In other words the gain at DC should not be infinity. This is conservative stability rule: because we must move 1500 kg of metal when we turn on our loops, such a high gain drive may be stressful on the actuators and the stability of the loop.
- With no low-frequency boost, we would like a phase margin of at least 40 deg at all frequencies below 20 Hz. Because we must move large amounts of mass, we ramp up the isolation loops from DC in a rather slow fashion. Hence, we want isolation loops to be unconditionally stable as the unity gain frequency sweeps from DC to frequencies near the designed UGF.
- Above 100 Hz, the open loop gain (OLG) should not rise above 0.2. This prevents any high frequency resonances from rearing their ugly heads unexpectedly.
- The sensitivity should never be greater than 3 at any frequency. This is simply because we want to keep gain peaking to a minimum. A related goal is to have the gain margin be around 4 or 5 dB.
- The low frequency boosted isolation loop may be only conditionally stable, as long as the 40 deg phase margin remains around the UGF.
- The low frequency boost should boost the gain at (and below) 0.1 Hz by at least 40dB (a factor of 100).

Other than these goals, we're free to design however we wish. In addition to the standard poles and zeroes, we use anything from notch filters, elliptic filters, gain bumps, etc. to achieve the above goals. Also note, that we also use the convention where there are no implicit minus signs in our loops. In other words, the sensitivity S is

$$S = \frac{1}{1-G}$$

where G is the open loop gain (If the controller is added with an implicit minus sign, G is positive denominator). This also means that the phase instability condition at UGFs occur at 0° instead of -180°.

2 Preliminary Results

In this section, we focus on the first performance measurements taken on June 27th 2008, with the H1 HAM6 ISI.

2.1 Blend filters

Figure 3 shows the blend filters that were used to obtain the performance. Note that each degree of freedom can in principle have independently shaped filters, optimized for a given chamber's payload. For these initial measurements, the filter shown below was used in all degrees of freedom. It important characteristics include a blend frequency of 0.2 Hz, with a notch at 0.73 Hz (the first X and Y translational resonances of the OMC double pendulum suspension).

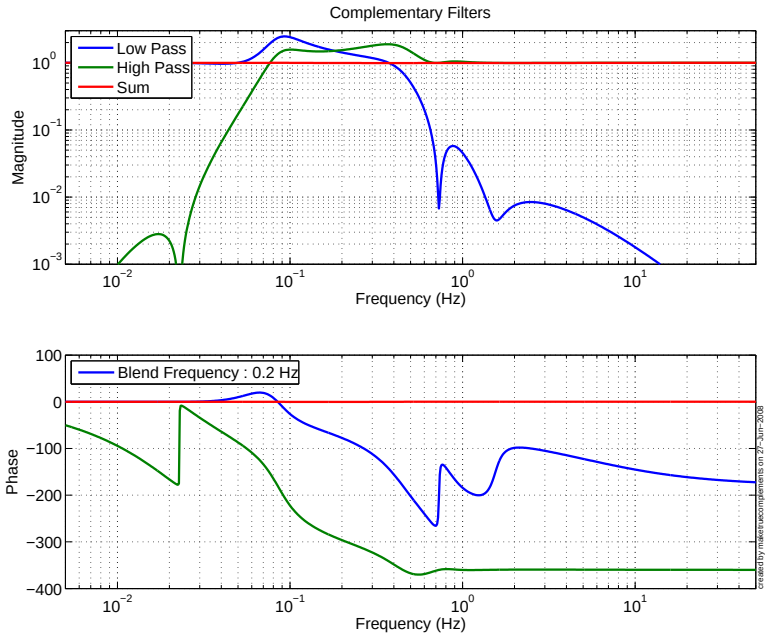

Figure 3: 0.2 Hz Blend filters used for performance measurements in Section 2.3.

2.2 Isolation Filters

Significant efforts made in the physical design of the HAM ISI to reduce cross-coupling between coordinate degrees of freedom. These efforts allow us to design the coordinate isolation filters in an entirely SISO manner. Hence this section describes the design of only the Y degree of freedom; the other degrees of freedom have been designed in a very similar manner, the results of which can be found in Appendix A.

Phase loss is one of the key components in control loop design. If the system to be controlled is flexible at all frequencies, having complicated resonance features near the desired unity gain

frequency, stable control is very difficult. The HAM ISI's physical system was built with this is mind, and therefore has been designed to be very stiff. Figure 4 shows the supersensor plant of the isolation control loop for the Y degree of freedom (aligned with the IFO light coming from the beam splitter).

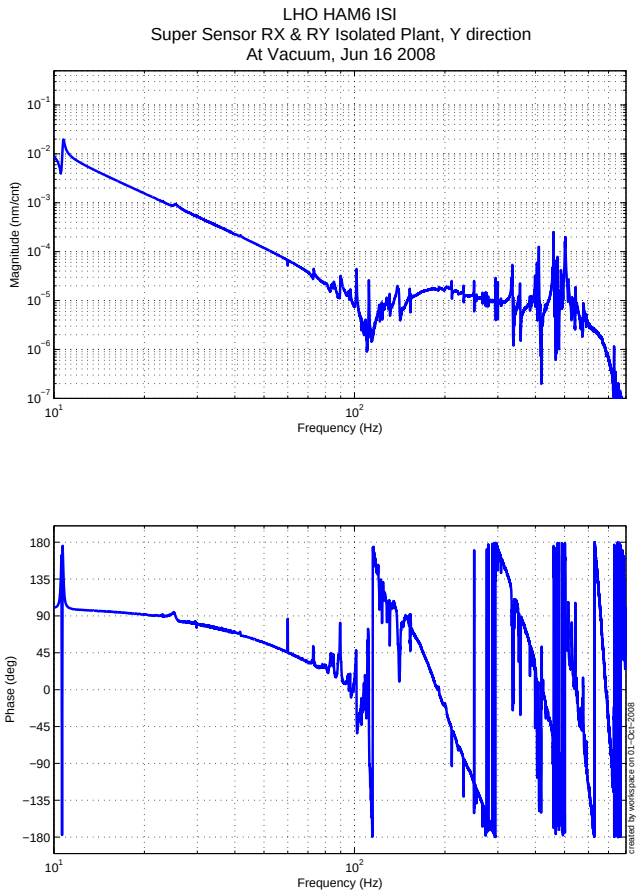

Figure 4: Super sensor isolation filter plant from 10 to 800 Hz.

Notice that the transfer function rolls off smoothly for two decades until around 100 Hz where we begin to see complications. (We save the support structure resonance at 11 Hz for discussion in Section 3.1). Above 100 Hz, we see two types of resonance features: high Q, sharp resonances and low Q, broad resonances. The former is easily compensated using a basic notch filter, which contributes a negligible amount of phase loss near the upper unity gain frequency. For the latter, one must use more sophisticated filters such as elliptic filters, which are more costly in phase. However, because of the stiff design, these broad resonance "forests" do not appear in the plant until very high frequencies which are well above the unity gain frequency. At such frequencies, we

can use the aggressive, high-phase-loss filters as necessary without significant effects on the loop stability. Hence, the isolation filters have a relatively simple shape and high unity gain frequencies.

Figure 5 shows several components of the filter design, with Figure 6 showing the same information but zoomed in around the unity gain frequency.

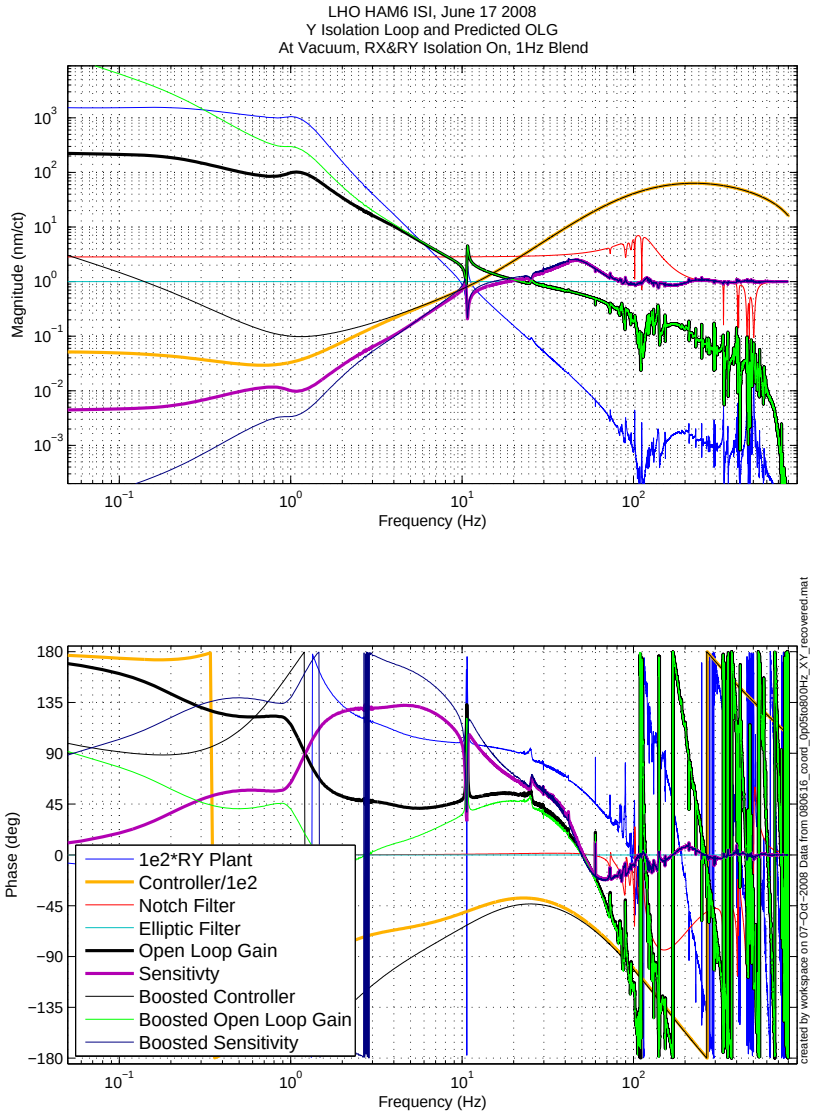

Figure 5: Example H1 HAM ISI isolation filter, open loop gain, and sensitivity for the Y degree of freedom.

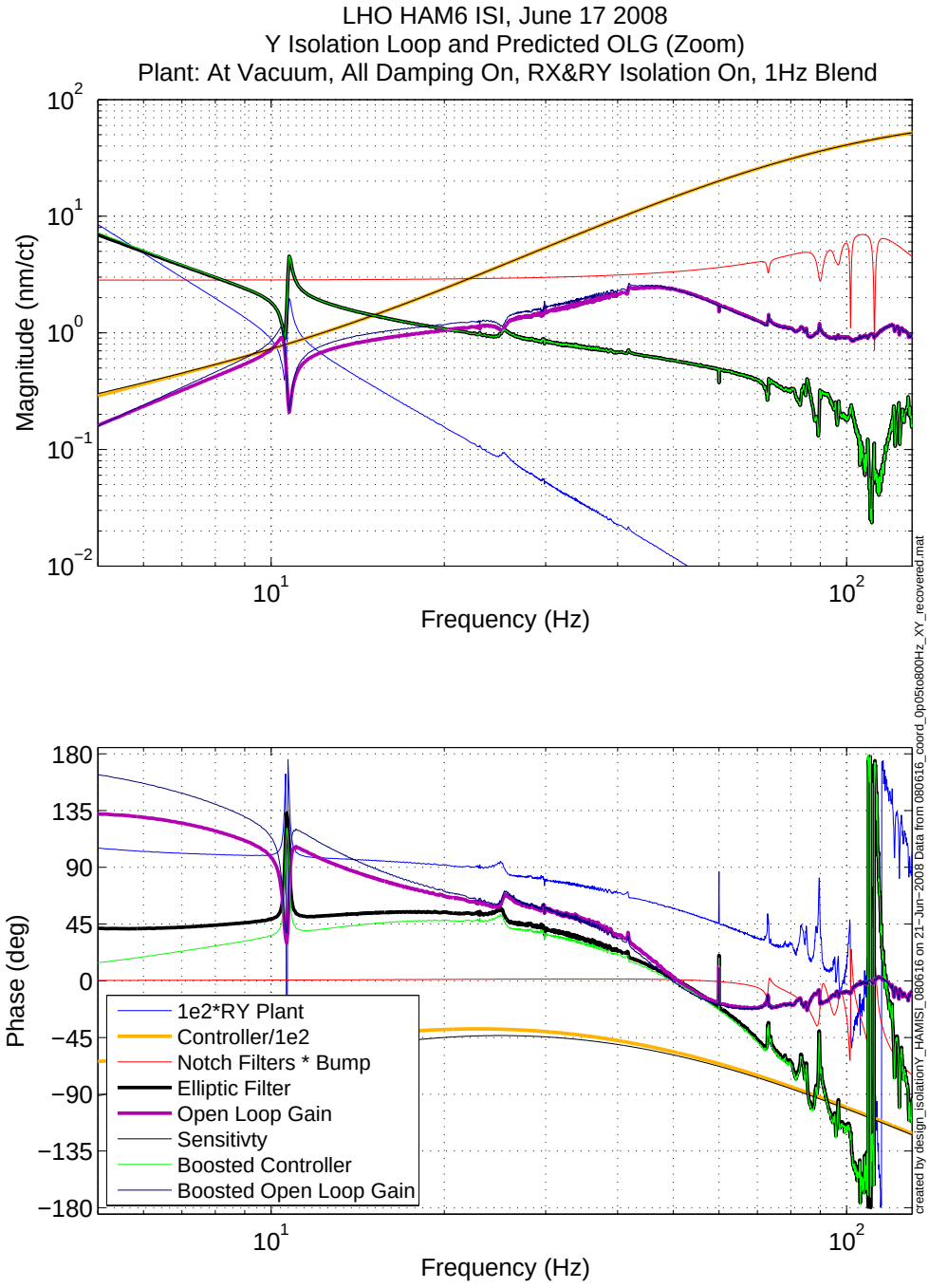

Figure 6: Zoom of the Y isolation filter, open loop gain, and sensitivity.

Shown in thin blue is the plant to be controlled (scaled by a factor of 100 such that is visible on the same scale as the rest of the curved in the plot), a portion of which we have already seen in Figure 4. The baseline isolation filter is shown in thick orange. For the Y degree of freedom, this consists of the following:

```
poles   : 0.25, 3, 45, pair(110,0), 300 [Hz]
zeroes : 0.6, pair(1,45), pair(12,30), 200 [Hz]
```

where `pair(amp,phase)` is a complex pair of poles or zeroes with an amplitude `amp`, and phase `phase`. These were chosen following the guidelines described in Section 1.1. To control high-frequency resonances, notches and additional poles and zeroes are added, which have been plotted separately in thin red for demonstrative purposes. The product of baseline and the high-frequency filters are used as the overall "controller," or isolation filter. The open loop gain, the product of the overall isolation filter (thick orange, and thin red) and the plant (thin blue), is shown in thick black (at high frequencies, thick black is overlapped by thin green). The sensitivity, which is a measure of the stability and performance of the closed loop system is shown in thick purple.

The low-frequency boost curves are shown as well, where the added boost filter changes the baseline isolation filter from thick orange to thin black; the open loop gain from thick black to thin green; and the sensitivity from thick purple to thin navy. The boost filter for the Y degree of freedom is

```
poles   : 0.01 3 [Hz]
zeroes : pair(3,30) [Hz]
```

I've chosen to use the Y degree of freedom as my example because it is the most important direction with respect to the interferometer, but it is crucial to note that is actually the degree of freedom with the lowest bandwidth. Table 1 summarizes the important information from the remainder of the degrees of freedom.

Table 1: Summary of isolation filter characteristics for H1's HAM6 ISI.

DOF	UGF [Hz]	Phase Margin [°]	Performance at 10Hz [ ]	Peak Sensitivity [ ]
X	27.0	37.70	0.4943	3.0406
Y	22.0	48.15	0.8512	2.6610
Z	25.0	42.10	0.4814	2.2245
RX	27.0	36.80	0.5043	2.9834
RY	28.0	35.00	0.4051	2.6785
RZ	28.0	35.70	0.4307	2.9646

Here, we can see we can achieve unity gain frequencies of up to 28 Hz, and virtually all of the design goals have been met. Again, see Appendix A for plots of each loops characteristics.

2.3 Displacement Performance

As of late June 2008, the isolation control loops have been closed on H1's HAM6 ISI. The results of these loops are shown in Figures 7-15, in both amplitude spectral densities (ASDs) and ground transmission.

The first six figures shown below are amplitude spectral densities of HAM ISI performance in displacement/rtHz. For these graphs, we recognize the orange displacement requirements from Section 1.2; the green curve demonstrates the passive performance (primarily above 1 Hz); and the blue curve shows the system with both damping and isolation loops on. The green and blue curves are taken with the in-loop GS-13 seismometers. For comparison, the red curve shows the ground motion adjacent to the chamber during the measurement, taken by a Streckheisen STS-2 seismometer.

First, we point out the significant isolation gained from the passive system alone. Above the translational resonances of the blade-spring/flexure system, we gain several orders of magnitude, such that we beat the Advanced LIGO requirements above 20 Hz. As expected, the active isolation yields performance between 0.5 Hz and 10 Hz. Where we do not meet the requirements below 0.5 Hz we expect to implement feed-forward sensor correction (see Section 3.2). The large feature we see between 10 and 15 Hz is a direct result of the support structure. This feature is discussed in detail in Section 3.1.

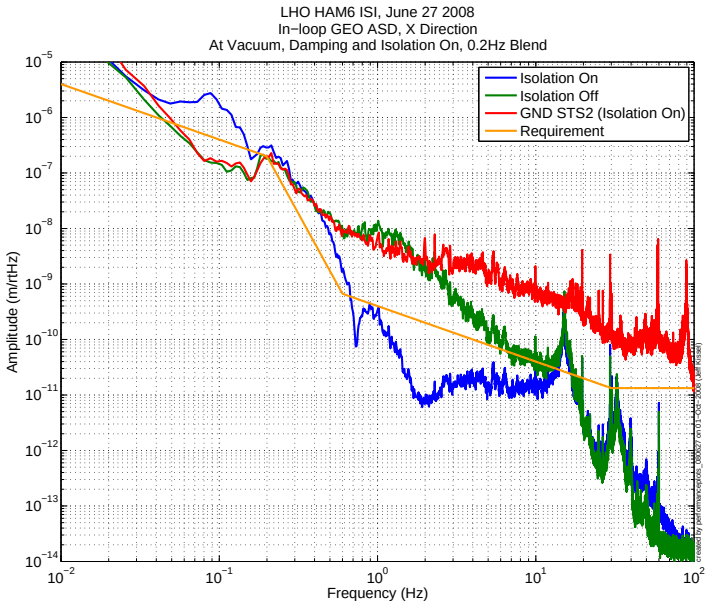

Figure 7: Preliminary isolation performance for the X degree of freedom.

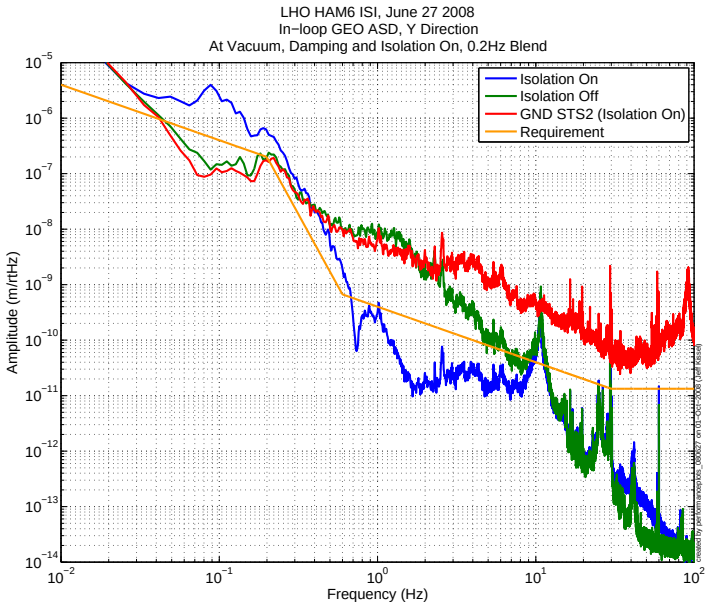

Figure 8: Preliminary isolation performance for the Y degree of freedom.

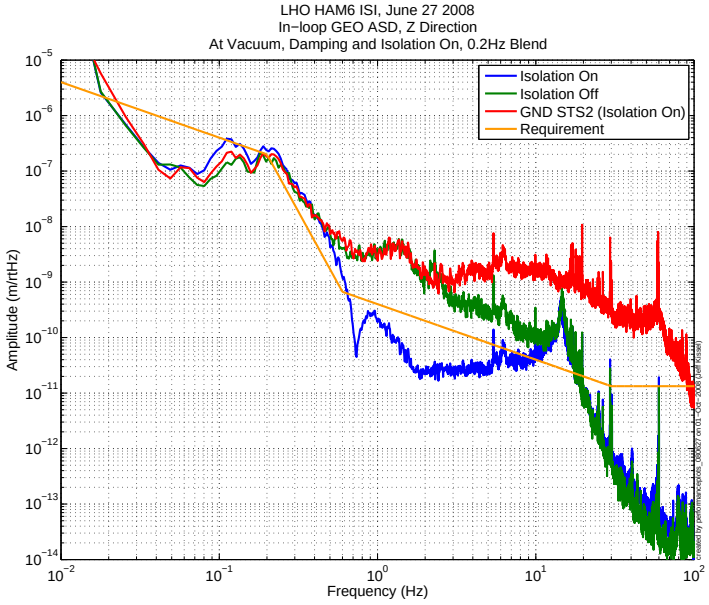

Figure 9: Preliminary isolation performance for the Z degree of freedom.

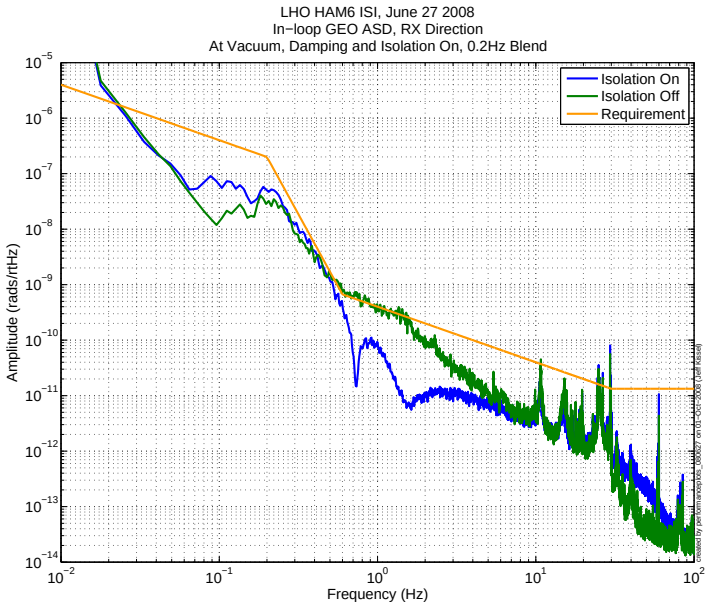

Figure 10: Preliminary isolation performance for the RX degree of freedom.

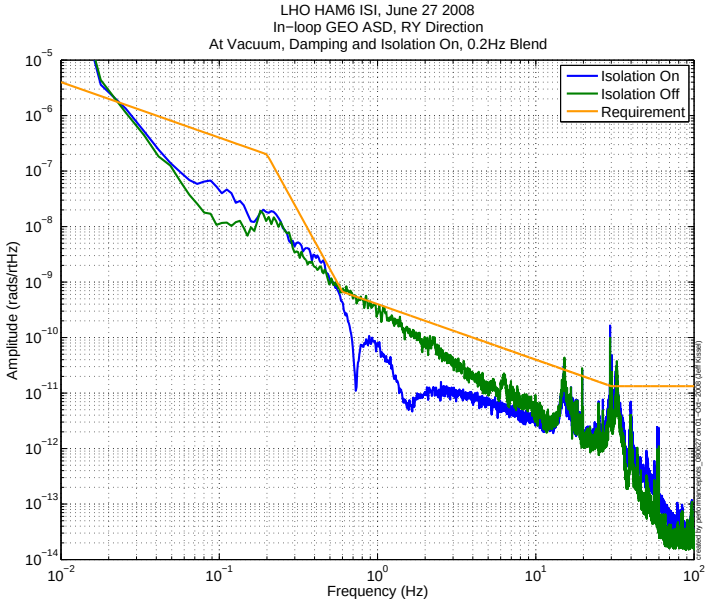

Figure 11: Preliminary isolation performance for the RY degree of freedom.

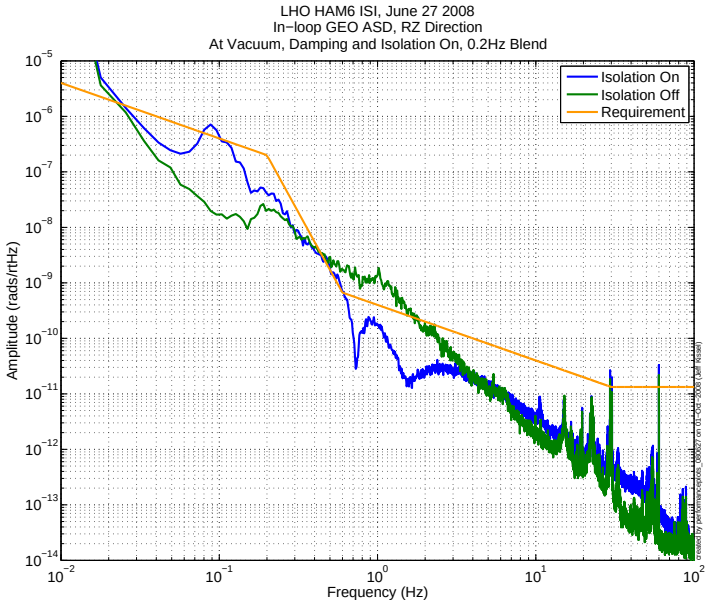

Figure 12: Preliminary isolation performance for the RZ degree of freedom.

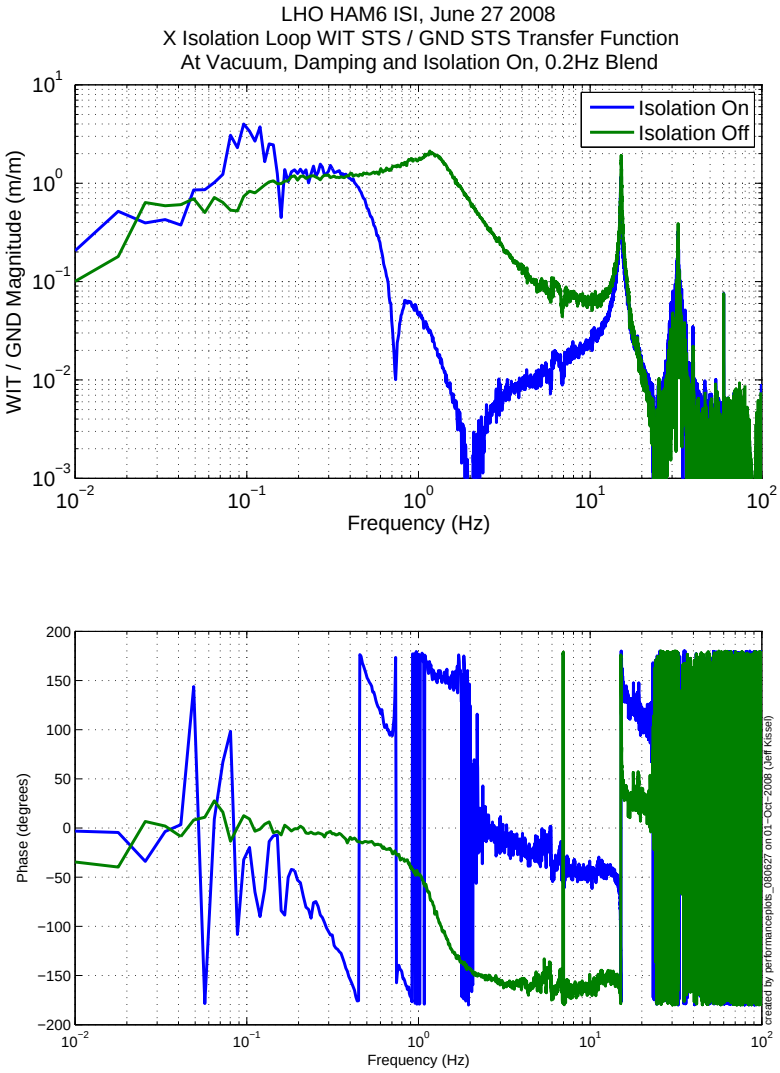

Figure 13: Preliminary ground transmission for the X degree of freedom.

Figures 13-15 show how ground motion is transmitted through the system. These transfer functions are between two STS-2 seismometers: one on the ground next to the HAM chamber, and the other resting on the HAM ISI optics table. The region of interest for these plots is between 0.1 Hz and 50 Hz; the surrounding data is contaminated by sensor noise. The dominant terms in the isolation performance (see [3] for details) are as follows

$$x_p = \frac{P_{x \leftarrow g_x}}{1-G}\, g_x + \frac{-G}{1-G}\, F_{disp,x} g_x + \frac{G}{1-G}\, F_{disp,x} F_{STS,x} g_x \quad (1)$$

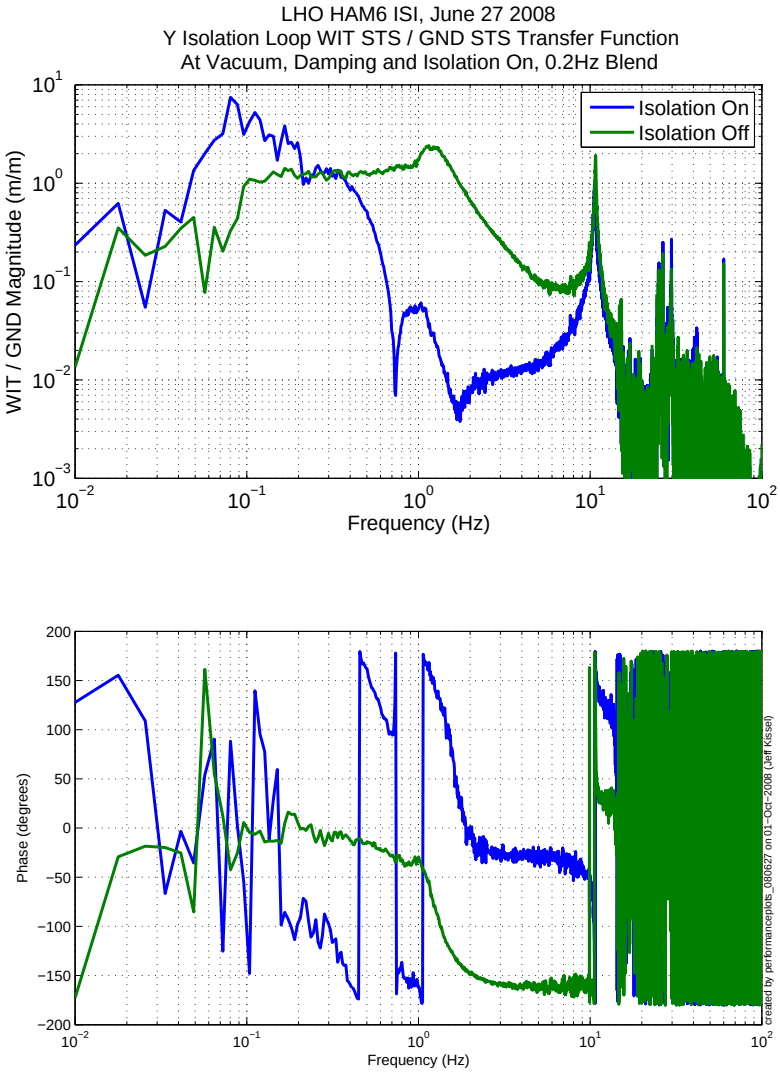

Figure 14: Preliminary ground transmission for the Y degree of freedom.

where x_p is he performance, g_x is the ground motion input into the system, $P_{x \leftarrow g_x}$ is the plant's transmission of ground without isolation, G is the open loop gain, $F_{disp,x}$ is the low-pass blend filter on the displacement sensors, and $F_{STS,x}$ is the low-pass sensor correction filter. Because these transmission plots were taken without sensor correction, we can ignore the third term. Hence all performance is gained by the plant's passive isolation (first term, shown in green), and ground motion transmitted through the displacement sensor blend filter, the sum of which is shown in blue.

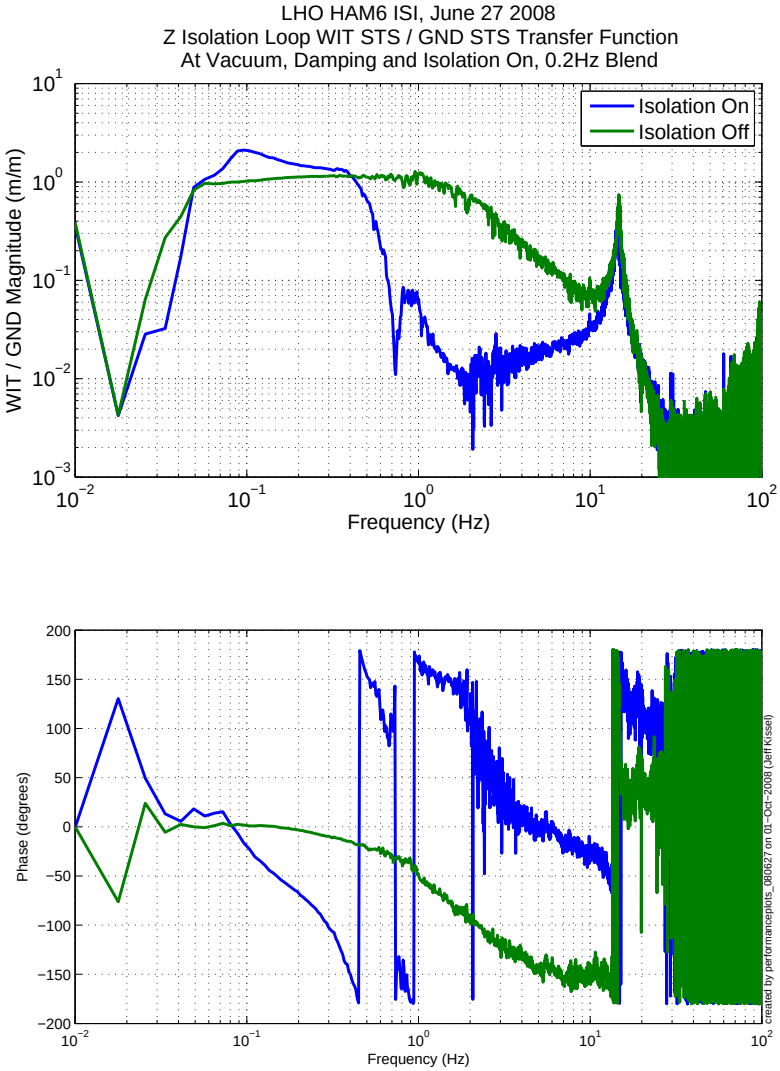

Figure 15: Preliminary ground transmission for the Z degree of freedom.

3 Improving the performance

In this section we will discuss future work on tuning and improving the isolation performance where Advanced LIGO requirements have not been met by the preliminary results from the prototypes.

3.1 Support structure resonance (Between 10 - 15 Hz)

One of the major issues with the performance measured on HAM6 is the large feature at 11.4 Hz which comes from a bending mode of the support structure. The support structure, or more specifically the "gull-wings" beams which grab the support tubes, has a Q of 50-100 resulting in table motion (for the H1 data) about a factor of 20 to 30 above the requirement. Simple calculations show that this feature should be dramatically reduced by the addition of new stiffer crossbeams and HEPI (described in [4]). These calculations are described in detail in the SEI log at `http://ligo.phys.lsu.edu:8080/SEI/1287`.

The new crossbeam is a little more than six times stiffer in the Y direction (parallel with the support tubes) than the gull-wing (see [4]). Without HEPI, this should more than double the frequency of the mode in the Y direction, but probably will not affect the damping in any way. However, the addition of HEPI actuators should add significant damping. The actuators have a built-in internal damping network, which is effective between about 8 Hz and 60 Hz. As a result of the increased stiffness in the new crossbeams, their compliance is smaller than the compliance of the HEPI actuators. Since the major compliance of the support structure is the damping portion of the actuators, the system will be well damped. A plot of the modeled stiffness of a single actuator is shown in Figure 17.

Figure 18 shows the result of our simple calculation, and compares the current situation (gull-wings without HEPI) to the Advanced LIGO configuration (new crossbeams and HEPI) and an intermediate condition (HEPI with gull-wings). We see that the performance in the Advanced LIGO configuration is quite good.

It is likely that the real situation will be somewhere between the modeled Advanced LIGO condition and the gull-wing with HEPI condition, because of additional, unmodeled compliance in the system. Thus, we expect that the real situation will probably have a peak around 12 Hz and a Q around 5. This is about a factor of 10 better than the situation now, but will probably still be slightly above the requirement. If we can get performance from HEPI at these frequencies, will have no problem meeting the requirements. If not, the table motion around 12 Hz may be slightly above the requirement curve. If this is a problem, one could investigate feedforward from the stage 0 structure to the isolation platform.

3.2 Sensor correction (Below 0.5 Hz)

For Enhanced LIGO, HAM 6 will have no external pre-isolation (HEPI) on its support structure. Therefore, feed-forward sensor correction will be implemented directly on the HAM ISI displacement sensors from a STS-2 positioned near the chamber. This method of implementation was the original design concept (discussed in [2]), and removes the intermediate tilt-translation coupling between gull-wing resonances. The control system will be a replica of what was developed by Wensheng Hua for the rapid prototype of the in-vacuum isolation systems.

Sensor correction removes ground coupling between translation motion as sensed by the displacement sensors. Since the displacement sensors only control the table up to the pre-determined blend frequency, it is below this frequency which we expect to see the most improvement in performance. However, because tilt couples into horizontal geophones inverse quadratically with respect

to frequency, we may get better performance from those sensors as well.

3.3 Blend filter tuning (Around and Below Blend Frequency

Technical noise may also contribute to inhibiting the performance of the HAM ISI. For example, sensor noise in the vertical seismometers can be misconstrued as differential motion. Differential motion of vertical seismometers produces excess tilt information, which then couples into horizontal translation decreasing performance for both X and Y degrees of freedom. This is evident in Figure **??**, a zoom the x translational performance. Also included is a model of how the GS-13 sensor noise behaves,

$$model \quad = \quad \frac{g}{\omega^2} \, F_{GS13,x} \, F_{GS13,ry} \, n_{GS13} \tag{2}$$

where G is the open loop gain, $F_{GS13,x}$ is the high-pass blend filter for the X degree of freedom, $F_{GS13,ry}$ is the high-pass blend filter for RY, and n_{GS13} is the measure noise of the GS-13 (projected to account for the three seismometer array).

This sensor noise coupling is dependent on the high-pass blend filters for X and RY. If they are tuned such that their gain rolls off significantly faster, or to have a less aggressive blend frequency, etc. this coupling can be reduced. This is just one example of the many ways that the design of the blend filters can be smarter; as mentioned in Section 2.1, the filters for each degree of freedom can be tuned independently. In this case, the same filters were naively placed over all degrees of freedom due to commissioning bugs and deadlines.

3.4 Changes in plant with payload (Above 100 Hz)

An important issue to keep in mind is that the control system must be modified when the payload on the table is modified. The modifications may be very simple, but it is necessary to re-measure the plant to prove this. We were able to demonstrate a rather extreme case of this on the H1 HAM6 ISI. In June 2008, the isolation filters were designed when the payload was an STS-2 in a pod on the center of the table, and dummy mass distributed on the table. Performance plots taken in June are with this payload. In August, the OMC suspension frame (and the OMC, and the steering mirrors, and the cables) were installed, the STS-2 removed, and the amount and position of dummy mass was adjusted to load and balance the table. The change in the plant is quite obvious. Below, in Figures 20 and 21, we plot the measured transfer function from the coordinate drive to super-sensor for RX and RY, the tip and tilt of the table. These measurements clearly show the bending modes of the OMC frame. Below 80 Hz, the transfer functions are nearly identical. Above 80 Hz, the general shape does not change, but several new modes appear.

One would expect the frame modes to couple strongly to these degrees of freedom of the table, and in the RX direction, they clearly do. To run a stable controller in the RX direction, about 5 new notches will need to be installed. Since there is no appreciable phase difference below 80 Hz, and the peaks are narrow, the implementation of these notches is a straightforward matter. If the computers are all working correctly, this type of control modification is a few days of work for someone with experience, to measure, design, implement, and test the 6 new controllers.

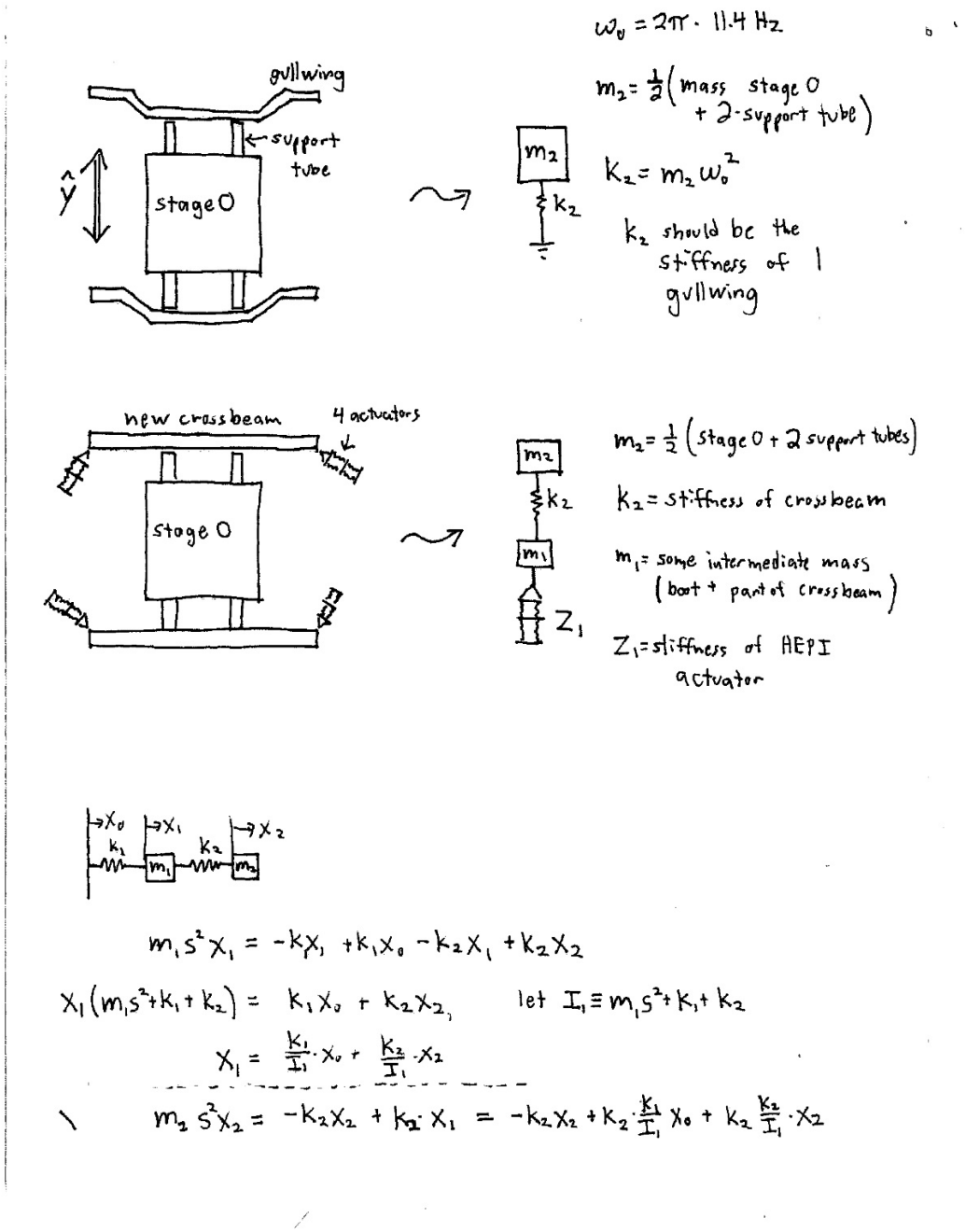

Figure 16: Schematic view of the simplified model used to evaluate the new crossbeams and HEPI on Advanced LIGO HAM systems.

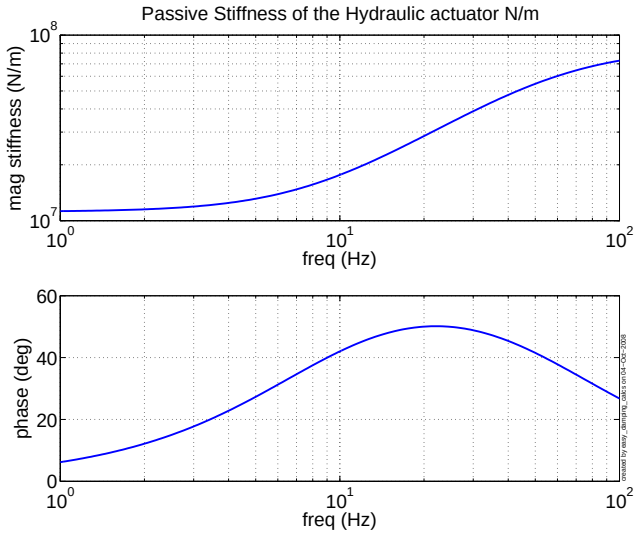

Figure 17: Passive stiffness of a HEPI actuator, showing the lossy nature of the actuator in the 10 - 50 Hz range which results from the internal damping network.

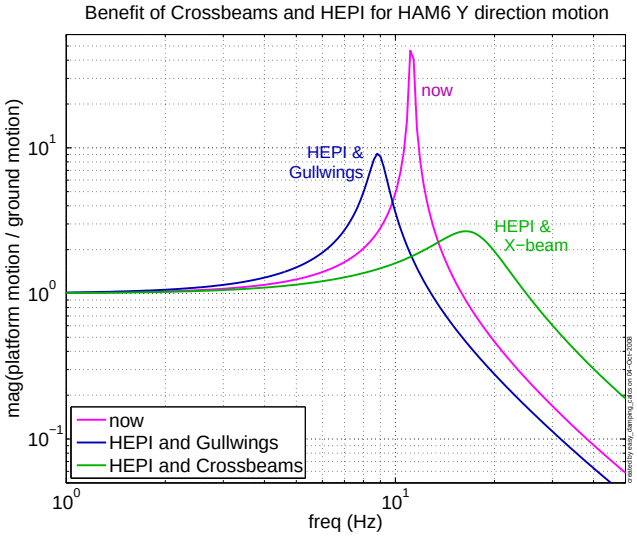

Figure 18: HEPI and the new crossbeam clearly improve the passive performance of the support structure by adding both stiffness and damping.

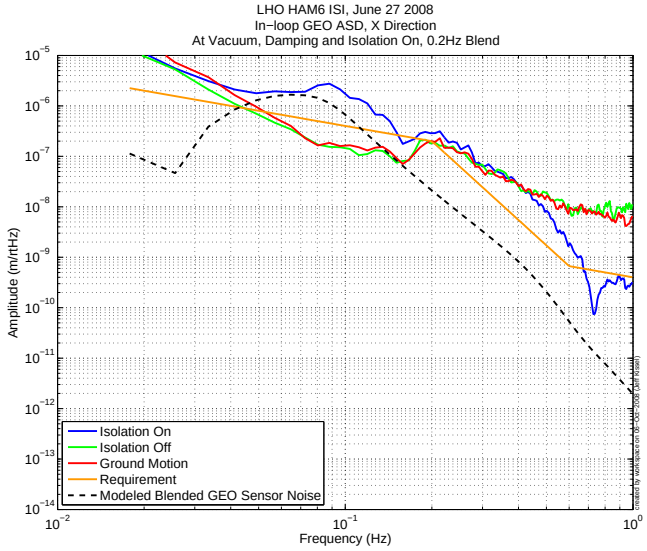

Figure 19: Low-frequency displacement performance for the X degree of freedom, with a model of the geophone sensor noise as tilt.

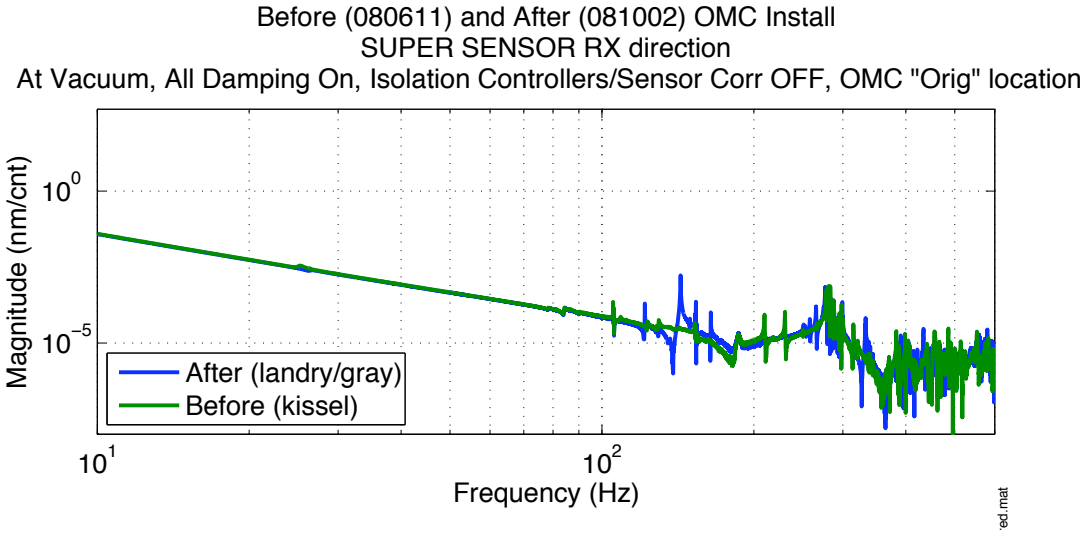

Figure 20: Measured transfer function of the H1 HAM6 in the RX direction (tilting back and forth towards the beamsplitter chamber) before and after the installation of the OMC suspension frame. The transfer function below 100 Hz is almost unchanged. Above 100 Hz, several new modes appear.

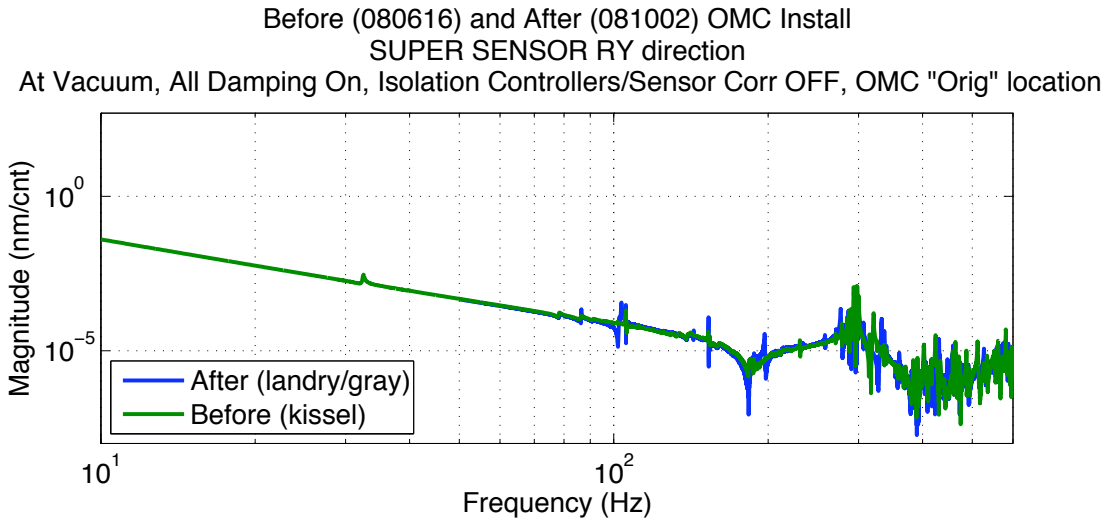

Figure 21: Measured transfer function in the RY direction (tipping transverse to the beam direction). Only a few new modes are visible here.

4 Conclusion

The Enhanced LIGO prototypes of the HAM ISI are well on the way to demonstrating its ability to meet or beat Advanced LIGO requirements. The results presented in Section 2 show excellent passive isolation above 15 Hz, reducing ground noise by factors of 50 or greater. The active control system has also demonstrated its worth, providing isolation of as much as a factor of 100 between 0.5 and 10 Hz. In addition to performance, prior effort in the design of the physical system has provided for a relatively painless experience molding the active control system. This will assist in the production-line style commissioning that must take place for Advanced LIGO. Finally, The improvements outlined in Section 3 should further improve its performance such that Advanced LIGO requirements are met at all frequencies.

References

[1] [P. Fritschel. **HAM seismic isolation requirements**. *LIGO-T060075-00* (2006)]

[2] [B. Lantz, Ken Mason, and the SEI Team. **Status report for the single stage HAM ISI for enhanced LIGO and advanced LIGO, april 2008**. *LIGO-T070088-00-R* (2007)]

[3] [B. Lantz. **Simple Calculation of Active Platform Performance.** *LIGO-T080119-00-R* (2008)]

[4] [A. Stein, S. Foley, K. Mason. **HAM Crossbeam Redesign for Advanced LIGO: Impact on HAM Chamber Placement.***LIGO-E080328-00-D* (2008)]

A X, Z, RX, RY, RZ, Isolation Filter Plots

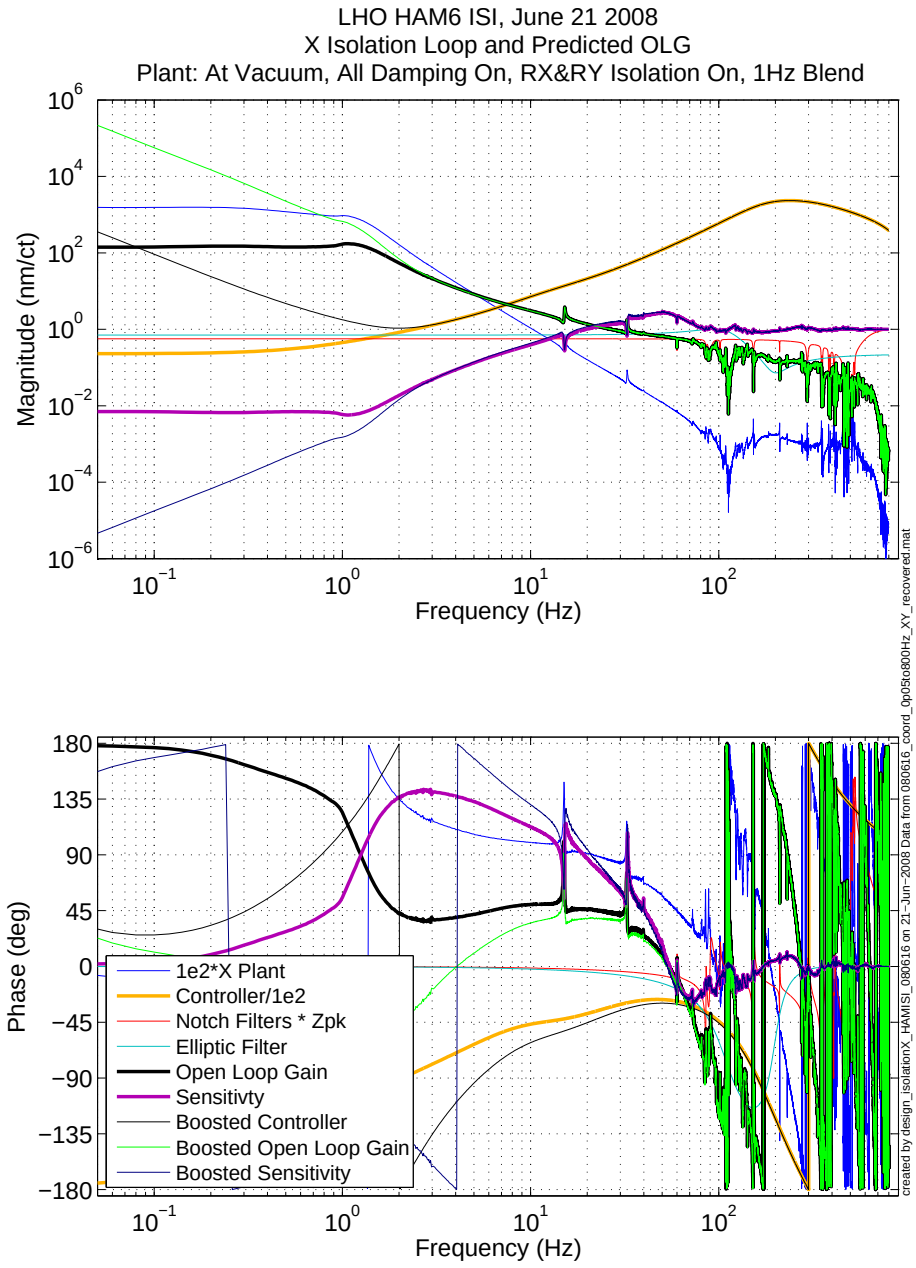

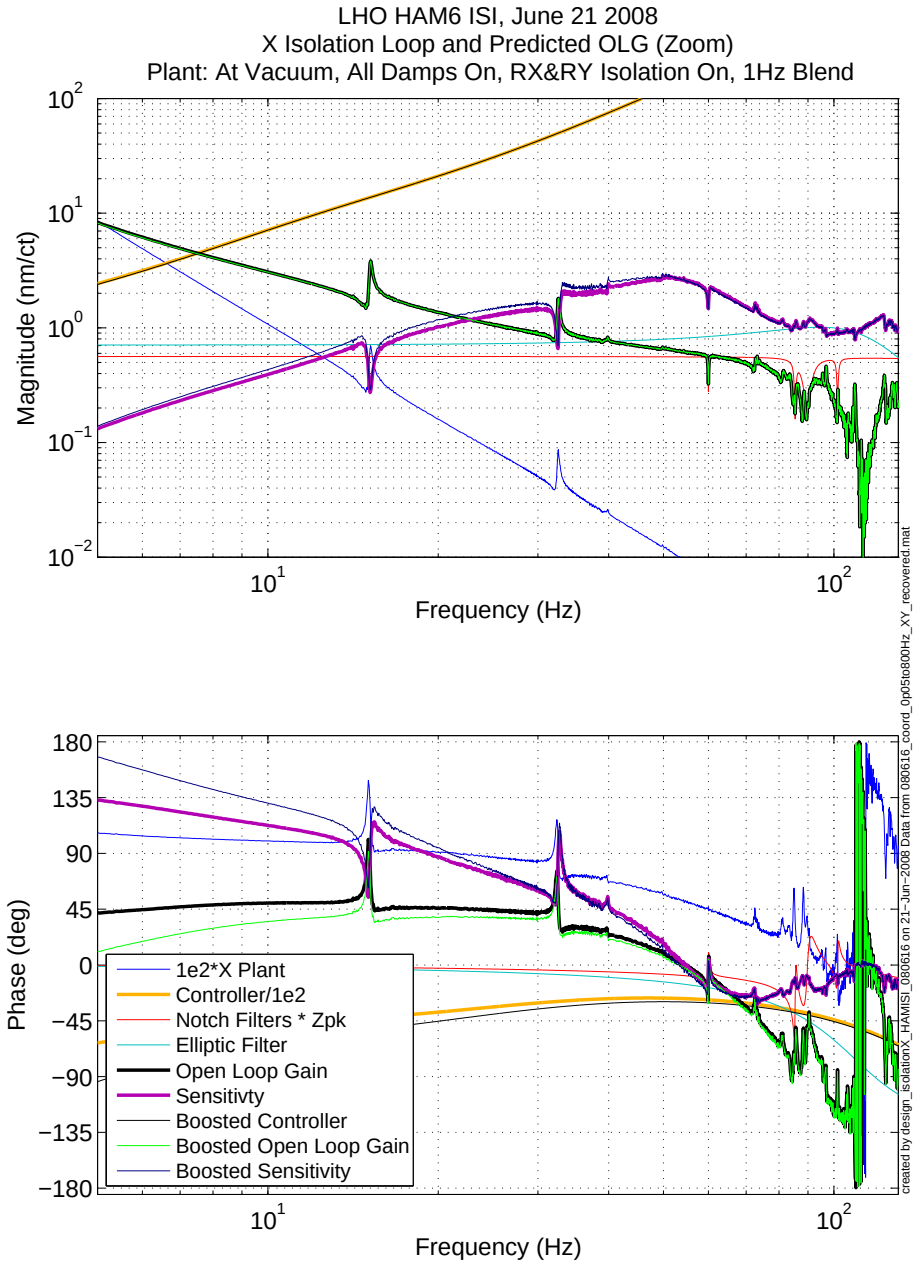
LHO HAM6 ISI, June 21 2008
X Isolation Loop and Predicted OLG (Zoom)
Plant: At Vacuum, All Damps On, RX&RY Isolation On, 1Hz Blend
Magnitude (nm/ct)
Frequency (Hz)
Phase (deg)
Frequency (Hz)
1e2*X Plant
Controller/1e2
Notch Filters * Zpk
Elliptic Filter
Open Loop Gain
Sensitivty
Boosted Controller
Boosted Open Loop Gain
Boosted Sensitivity
created by design_isolationX_HAMIS1_080616 on 21−Jun−2008 Data from 080616_coord_0p05to800Hz_XY_recovered.mat

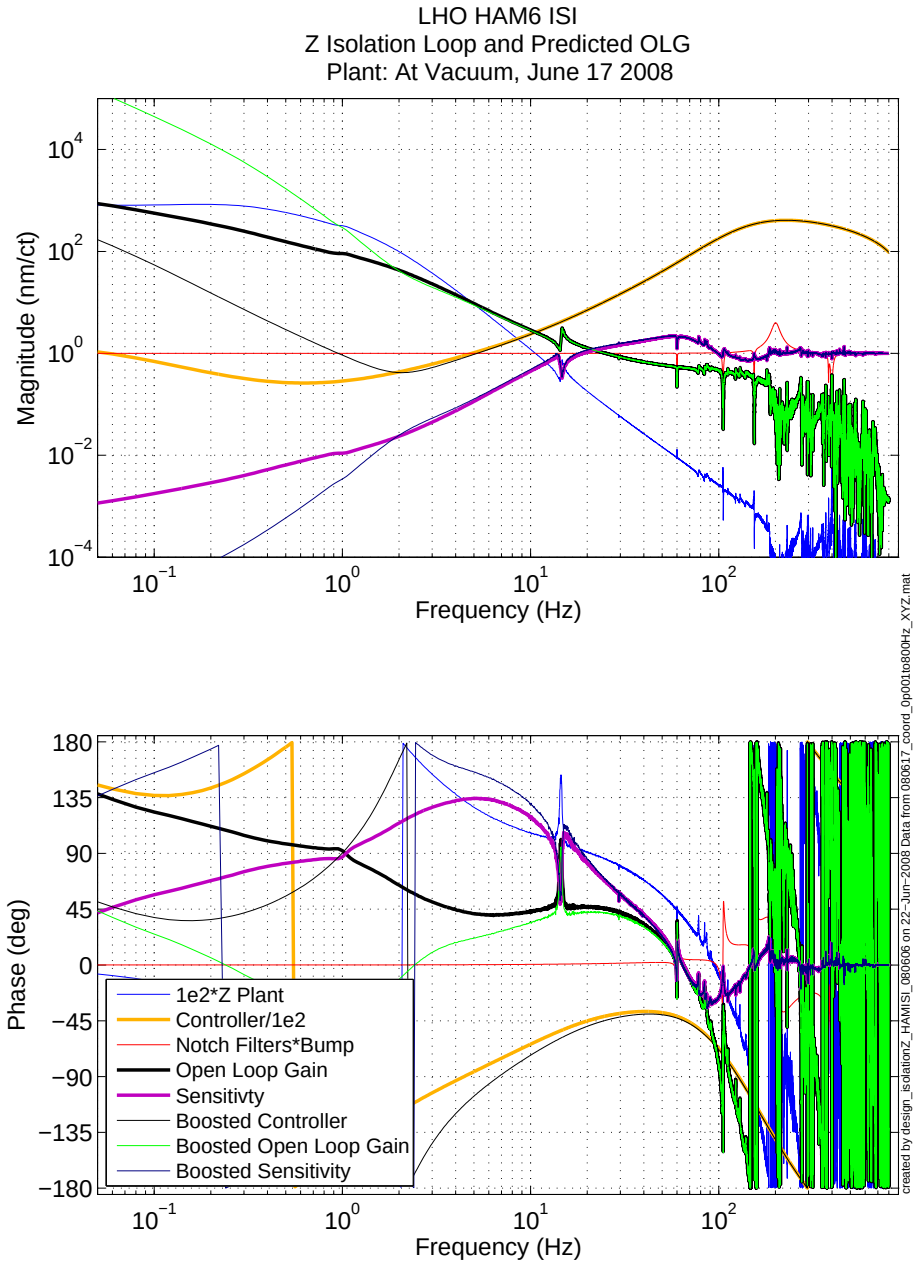
LHO HAM6 ISI
Z Isolation Loop and Predicted OLG
Plant: At Vacuum, June 17 2008
Magnitude (nm/ct)
Frequency (Hz)
Phase (deg)
Frequency (Hz)
1e2*Z Plant
Controller/1e2
Notch Filters*Bump
Open Loop Gain
Sensitivty
Boosted Controller
Boosted Open Loop Gain
Boosted Sensitivity
created by design_isolationZ_HAMIS1_080606 on 22−Jun−2008 Data from 080617_coord_0p001to800Hz_XYZ.mat

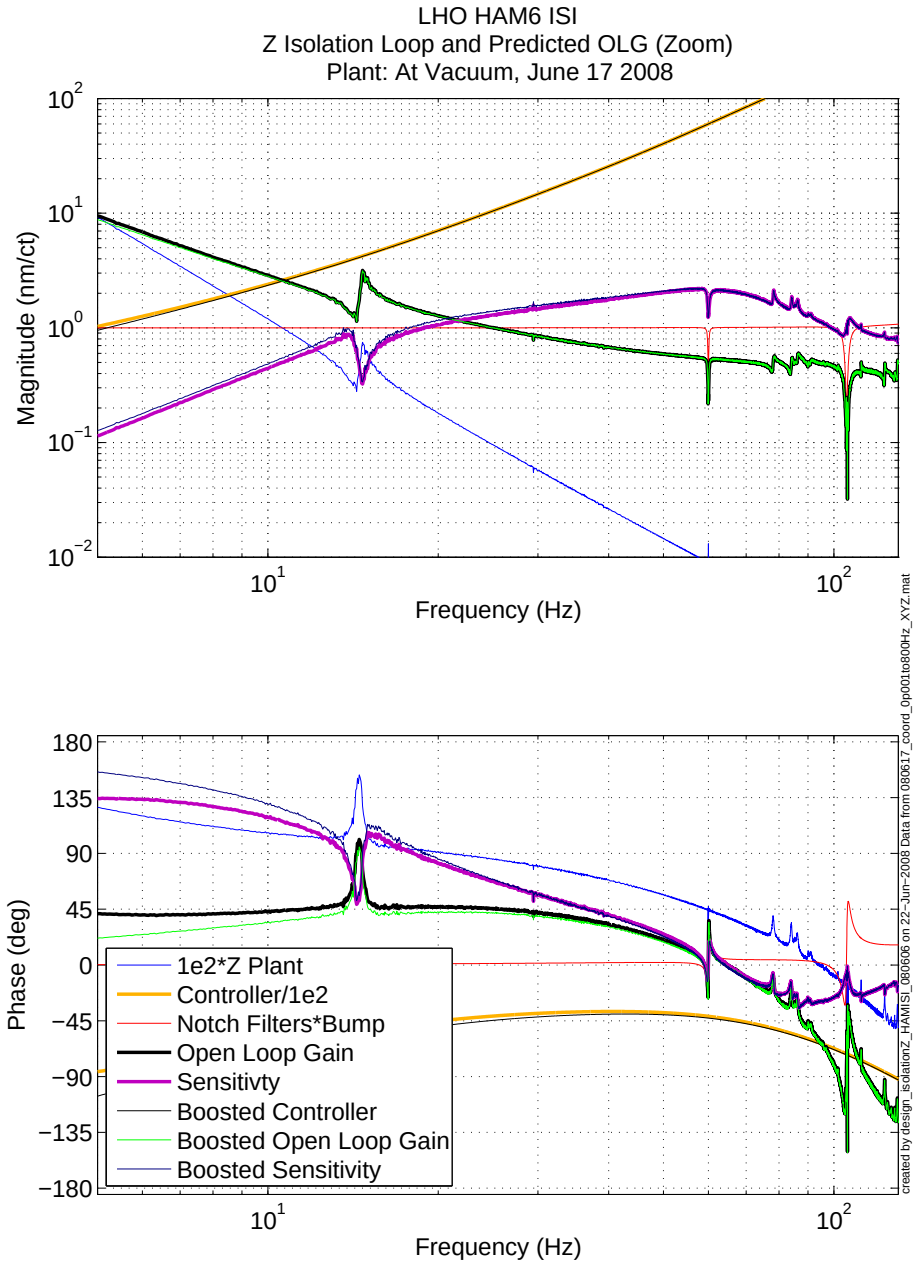
LHO HAM6 ISI
Z Isolation Loop and Predicted OLG (Zoom)
Plant: At Vacuum, June 17 2008
Magnitude (nm/ct)
Frequency (Hz)
Phase (deg)
Frequency (Hz)
1e2*Z Plant
Controller/1e2
Notch Filters*Bump
Open Loop Gain
Sensitivty
Boosted Controller
Boosted Open Loop Gain
Boosted Sensitivity
created by design_IsolationZ_HAMISI_080606 on 22−Jun−2008 Data from 080617_coord_0p001to800Hz_XYZ.mat

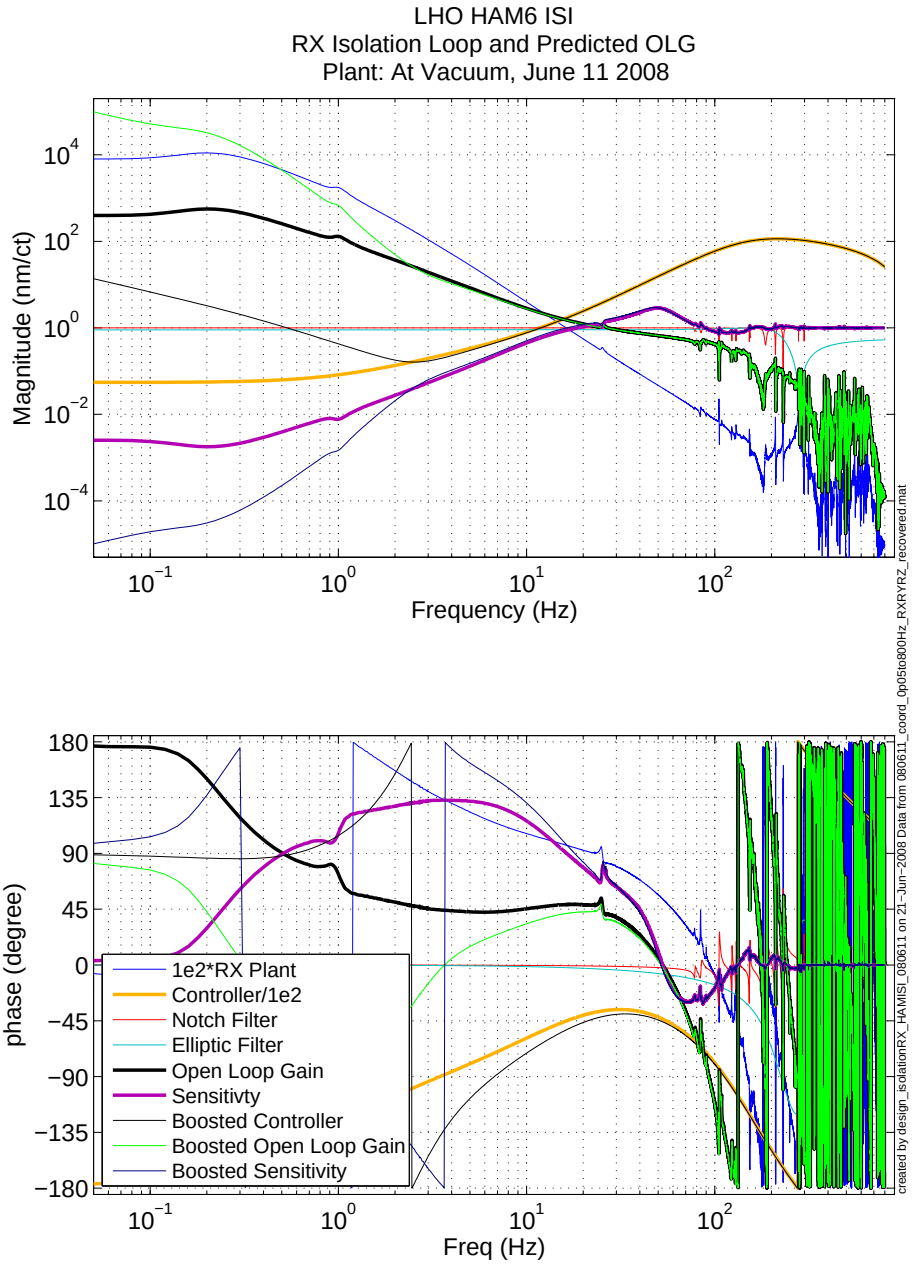
LHO HAM6 ISI
RX Isolation Loop and Predicted OLG
Plant: At Vacuum, June 11 2008
Magnitude (nm/ct)
Frequency (Hz)
phase (degree)
Freq (Hz)
1e2*RX Plant
Controller/1e2
Notch Filter
Elliptic Filter
Open Loop Gain
Sensitivty
Boosted Controller
Boosted Open Loop Gain
Boosted Sensitivity
created by design_isolationRX_HAMISI_080611 on 21−Jun−2008 Data from 080611_coord_0p05to800Hz_RXRYRZ_recovered.mat

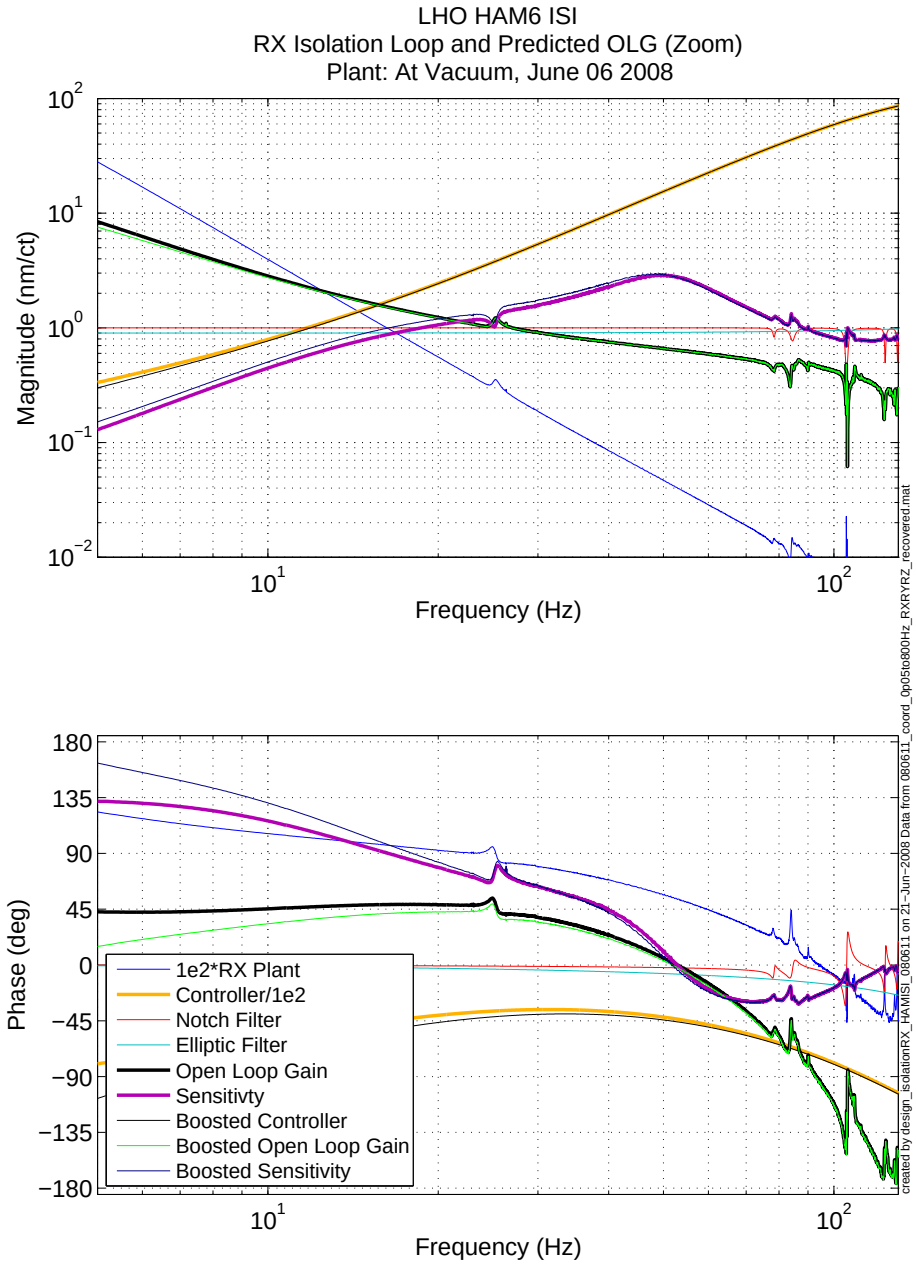
LHO HAM6 ISI
RX Isolation Loop and Predicted OLG (Zoom)
Plant: At Vacuum, June 06 2008
Magnitude (nm/ct)
Frequency (Hz)
Phase (deg)
Frequency (Hz)
1e2*RX Plant
Controller/1e2
Notch Filter
Elliptic Filter
Open Loop Gain
Sensitivty
Boosted Controller
Boosted Open Loop Gain
Boosted Sensitivity
created by design_IsolationRX_HAMISI_080611 on 21−Jun−2008 Data from 080611_coord_0p05to800Hz_RXRYRZ_recovered.mat

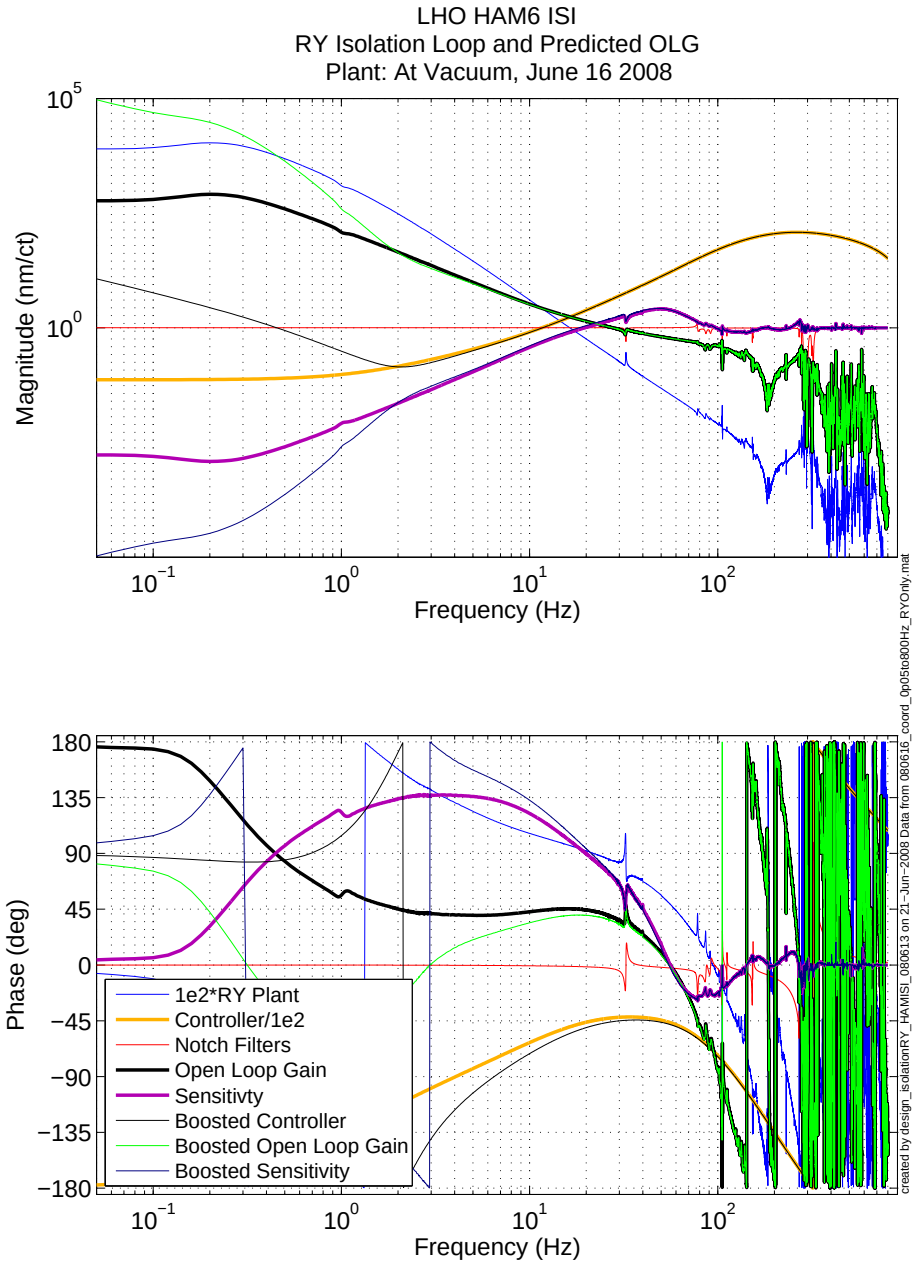
LHO HAM6 ISI
RY Isolation Loop and Predicted OLG
Plant: At Vacuum, June 16 2008
Magnitude (nm/ct)
Frequency (Hz)
Phase (deg)
Frequency (Hz)
1e2*RY Plant
Controller/1e2
Notch Filters
Open Loop Gain
Sensitivty
Boosted Controller
Boosted Open Loop Gain
Boosted Sensitivity
created by design_isolationRY_HAMISI_080613 on 21−Jun−2008 Data from 080616_coord_0p05to800Hz_RYOnly.mat

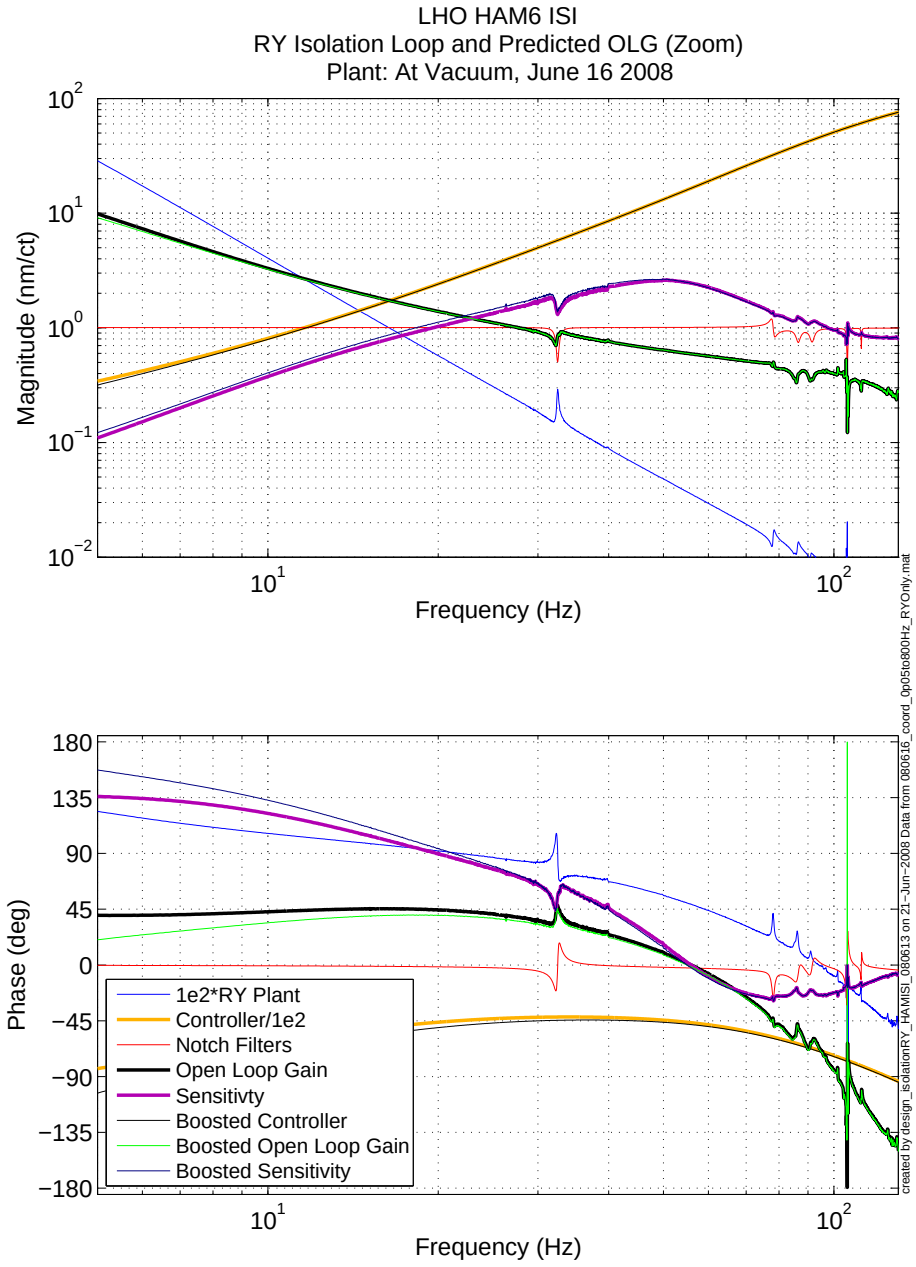
LHO HAM6 ISI
RY Isolation Loop and Predicted OLG (Zoom)
Plant: At Vacuum, June 16 2008
Magnitude (nm/ct)
Frequency (Hz)
Phase (deg)
Frequency (Hz)
1e2*RY Plant
Controller/1e2
Notch Filters
Open Loop Gain
Sensitivty
Boosted Controller
Boosted Open Loop Gain
Boosted Sensitivity
created by design_IsolationRY_HAMISI_080613 on 21−Jun−2008 Data from 080616_coord_0p05to800Hz_RYOnly.mat

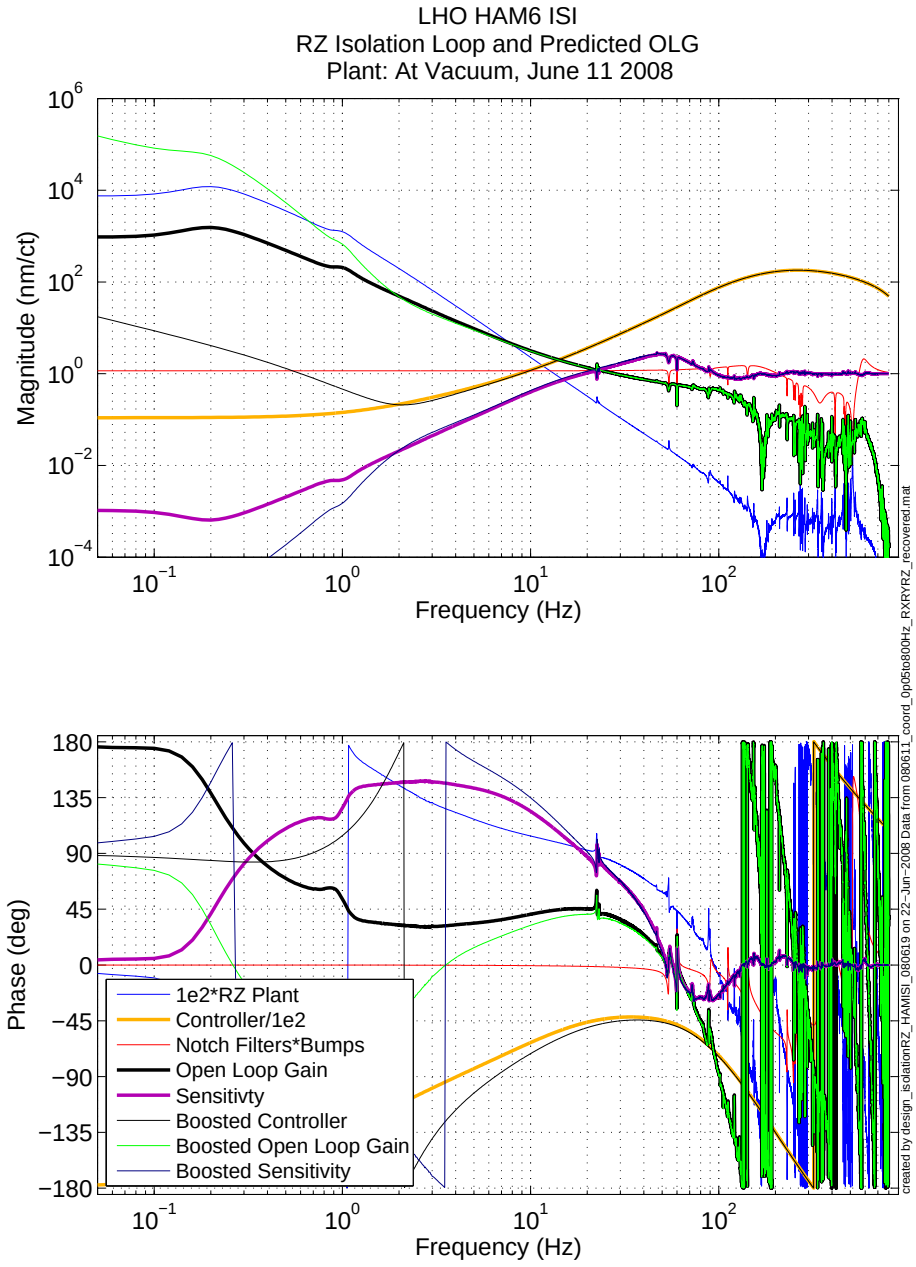
LHO HAM6 ISI
RZ Isolation Loop and Predicted OLG
Plant: At Vacuum, June 11 2008
Magnitude (nm/ct)
Frequency (Hz)
Phase (deg)
Frequency (Hz)
1e2*RZ Plant
Controller/1e2
Notch Filters*Bumps
Open Loop Gain
Sensitivty
Boosted Controller
Boosted Open Loop Gain
Boosted Sensitivity
created by design_isolationRZ_HAMISI_080619 on 22−Jun−2008 Data from 080611_coord_0p05to80Hz_RXRYRZ_recovered.mat

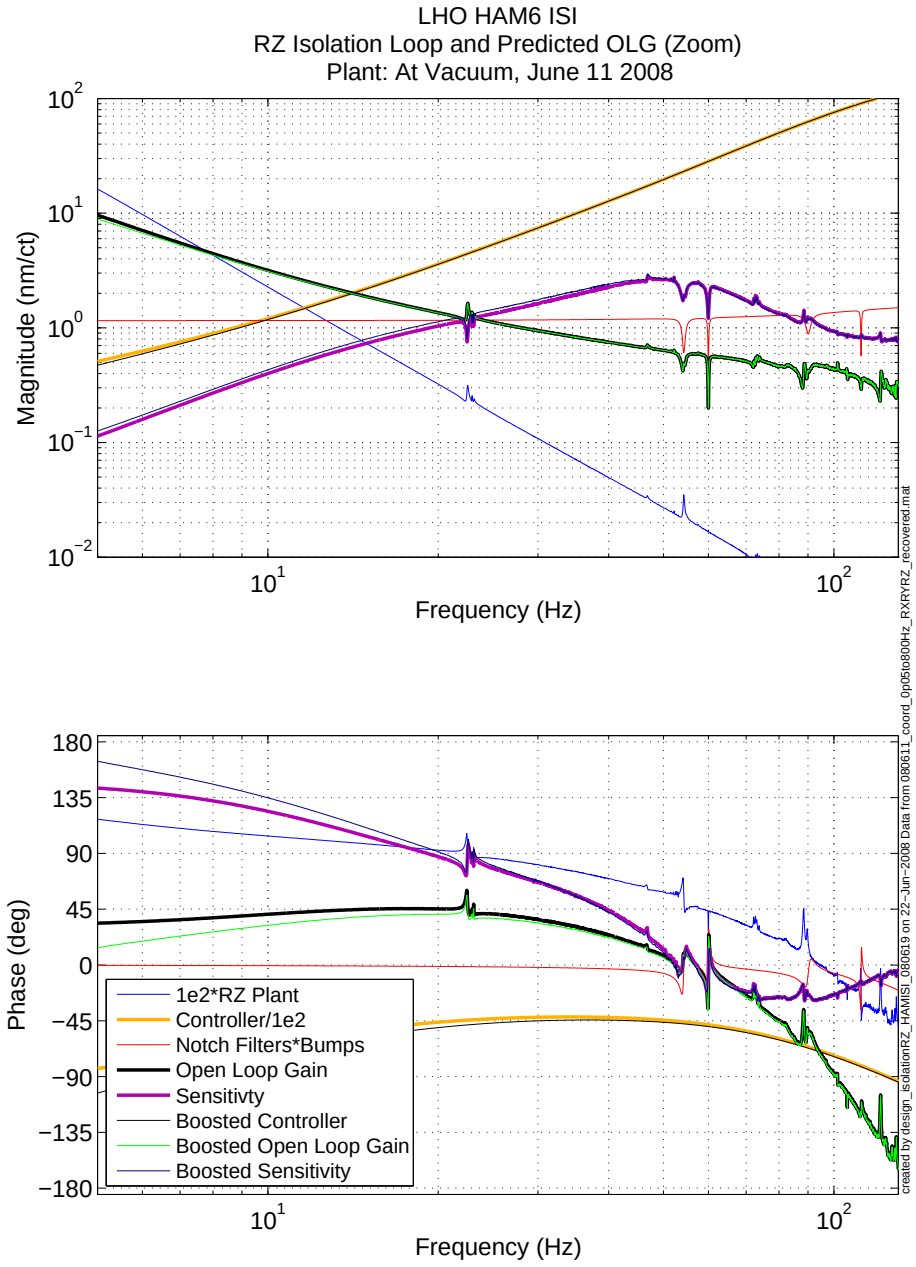
LHO HAM6 ISI
RZ Isolation Loop and Predicted OLG (Zoom)
Plant: At Vacuum, June 11 2008
Magnitude (nm/ct)
Frequency (Hz)
Phase (deg)
Frequency (Hz)
1e2*RZ Plant
Controller/1e2
Notch Filters*Bumps
Open Loop Gain
Sensitivty
Boosted Controller
Boosted Open Loop Gain
Boosted Sensitivity
created by design_isolationRZ_HAMISI_080619 on 22−Jun−2008 Data from 080611_coord_0p05to800Hz_RXRYRZ_recovered.mat